Assisted Spatial Sit-to-Stand Prediction-Part 1: Virtual Healthy Elderly Individuals

James Yang[1]
Fellow ASME
Human-Centric Design Research Lab,
Department of Mechanical Engineering,
Texas Tech University,
Lubbock, TX 79409
e-mail: james.yang@ttu.edu

Burak Ozsoy
Department of Mechanical Engineering,
Texas Tech University,
Lubbock, TX 79409
e-mail: burakozsoy@gmail.com

Sit-to-stand (STS) motion is a key determinant of functional independence for the senior people. This paper extends a predictive dynamics formulation previously reported to predict the assisted STS motion, i.e., the motion with a mechanical assistance, unilateral grab-rail bar which is placed on the right side of the virtual-individuals with a vertical orientation. The formulation is able to predict kinetics and kinematics not only in the sagittal plane, but also in frontal and transverse planes. Two different objective functions are tested: The first one is the dynamic effort and the second one is the dynamic effort plus the difference between right and left side support reaction forces (SRFs). Results show that sagittal plane kinematics and kinetics are not affected by the introduction of the grab-rail bar, whereas some significant differences are seen in the medial/lateral and anterior/posterior components of kinematics and kinetics. The healthy elderly group places a priority to the stability during an assisted STS task. The placement of the grab-rail bar on the right side results in a significant decrease in the left knee joint torque. Results in this study are consistent with those reported from the literature. [DOI: 10.1115/1.4048128]

Keywords: sit-to-stand (STS), assisted STS, optimization, predictive dynamics, human computer interfaces/interactions, physics-based simulations

1 Introduction

In 1987, it was estimated that more than 2 million of the elderly in U.S. had difficulties in accomplishing sit-to-stand (STS) tasks [1]. Many of the elderly were unable to rise from a chair without assistance [2]. Although there is no recent data, the population age 65 and over increased from 37.2 million in 2006 to 49.2 million in 2016 (a 33% increase) and is projected to almost double to 98 million in 2060 according to the [3]. A mechanical support is the most common solution for this issue. That is to say, many elderly prefer to use grab-rail bars to overcome the difficulty during standing up from a chair. O'Meara and Smith [4] studied the effects of unilateral grab-rail assistance on the STS performance of healthy elderly people. It was concluded that the introduction of the grab-rail bar brings asymmetry to the joint coordination even for healthy subjects. They also suggested placing the grab-rail bar at the opposite side of the injured side. In reality, this is not always the case. The performance of an elderly individual with a knee injury and receiving assistance from a grab-rail bar at the same side of the injury is still not clear.

Based on Riley et al. [5], the STS motion has four stages: (1) the flexion momentum stage, where the upper body rotates, moving the center of mass (CoM) location forward and slightly downward; (2) the transition between horizontal and vertical momentum; (3) the extension stage where the vertical component of the CoM location rises; and (4) motion finalization with stabilization. The most demanding instance of the STS task is the seat-off instance (in stage 2) where the body loses contact with the chair, the posture is often statically unbalanced with the CoM position located posterior to the heel and outside of the support region [6,7].

Significant research work has been done in unassisted STS task in the literature. Experimental method has been implemented to investigate influential factors of STS tasks: speed [1,8–10], muscle strength [6,10–12], postural stability [9,13,14], symmetry [15–18], chair height [19–24], arm support [2,4,23–26], age [2,6,10,11,19,27–29], feet locations at seat-off instance [16,20,21,30], injury and joint replacements [31–34], neurological disorders [35,36], obesity [37], and pregnancy [17,18,38]. Limited studies related to the simulation of STS tasks are reported in the literature and they are either dependent on experimental data, mostly consider the STS task of subjects only in 2D or the task starts after the seat-off instance [39,40]. Norman-Gerum and McPhee [41] reported a 2D STS motion prediction based on Bezier curves and validated the model through experiments. Another simulation-based model was introduced where healthy young people and amputees were examined in 3D [42]. Although standing-up trajectories were synthesized for healthy young subjects and amputees through dynamic optimization, the initial time of the motion was considered to be the seat-off instance. Mughal and Iqbal [43] developed optimal controllers for 3D STS and studied neuromuscular disorders by decoupling intact and neurodeficient extremities with the reference experimental trajectories. Robert et al. [44] reported an inverse dynamics method through optimization during a STS to estimate external contact loads but the method can only estimate unmeasured external loads with the given kinematics. In summary, none of the aforementioned methods in the literature can be easily adapted to study cause and effect in 3D space or is capable of predicting the performance during an STS maneuver without experimental data.

In our recent work, a three-dimensional unassisted sit-to-stand motion prediction was reported and applied to virtual young and elderly individuals [45]. However, it did not consider hand supports from the assistive device, such as grab-rail support. The present paper extends the STS formulation without hand assistive device to predict the assisted STS motion involving a mechanical support from a grab-rail bar placed on the right side of the elderly individual by adding the support forces as extra design variables.

2 Methodology

2.1 Digital Human Model. The elderly individuals are considered to receive help from a grab-rail bar placed on the right side of the body. Therefore, the elderly's right arm, shoulder and clavicle, trunk, and all lower extremities are involved in the digital human model, making the total number of active degrees

[1]Corresponding author.

Manuscript received February 13, 2020; final manuscript received July 19, 2020; published online February 9, 2021. Assoc. Editor: Caterina Rizzi.

of freedom (DOFs) 30 shown in Fig. 1. STS motions are predicted for five male and five female virtual-individuals with statures (1.58–1.87 m, mean = 1.71 m, SD = 0.09 m), and mass (47.8–81.9 kg, mean = 66.6 kg, SD = 11.6 kg). For each virtual-individual, link lengths are directly taken from the database [46], where link masses, center of mass locations, and inertia parameters are obtained through regression equations [47].

2.2 Optimization Formulation. In this section, the mathematical formulation of the assisted STS motion prediction problem is explained. The formulation is constructed as a nonlinear optimization problem with design variables, objective function, and constraints.

2.2.1 Design Variables. For the assisted STS motion prediction, the design variable vector is composed of control points, a knot vector that take place in the prediction of joint trajectories, and the unknown support reaction forces (SRFs) at the right hand in anterior/posterior (A/P), vertical, and medial/lateral (M/L) directions. The unknown SRF profiles at the right hand are discretized with quartic B-splines as well as joint trajectories. The design variable vector, ${}^{\xi}\mathbf{x}$, can be defined as

$$ {}^{\xi}\mathbf{x} = [(\mathbf{P}_i^j)^T,\ (\mathbf{R}_i^u)^T,\ (\mathbf{t}_k)^T]^T \tag{1} $$

where $\mathbf{P}_i^j$ is the vector of control points for the prediction of joint trajectories, $\mathbf{R}_i^u$ is the vector of control points for the prediction of SRFs at the right hand, $\mathbf{t}_k$ is the vector of knots, $i = 1, \ldots, 8$, $j = 1 \ldots 30$, $u = 1, 2, 3$, and $k = 1, 2, 3$. The total number of design variables is 267 (8*30 + 8*3 + 3).

2.2.2 Objective Function. For 3D STS motion prediction without hand support [45], two terms, i.e., dynamic effort and the difference in the vertical SRFs between the right and left side of the body, were considered in the objective function as in Eq. (3). However, the introduction of a grab-rail support causes asymmetry for the whole body joint coordination in the STS motion [4,48]. Therefore, two different objective functions will be tested in this study, as shown in Eqs. (2) and (3)

$$ \text{Obj}_1 = \text{minimize: } f_{Torque} \tag{2} $$

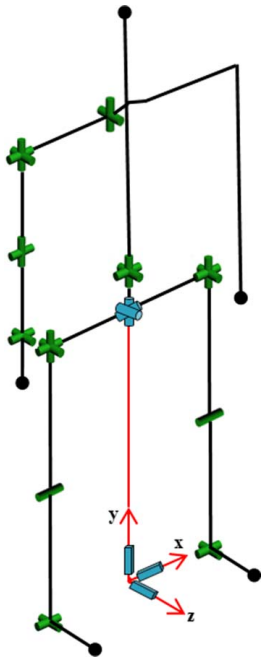

Fig. 1 30-DOF digital human model template

$$ \text{Obj}_2 = \text{minimize: } f_{Torque} + f_{SRF} \tag{3} $$

where

$$ f_{Torque} = \int_{t=0}^{t_f} \sum_{i=7}^{n} \left(\frac{\tau_i(\mathbf{q}, \dot{\mathbf{q}}, \ddot{\mathbf{q}}, t)}{\tau_i^{\lim}} \right)^2 dt \tag{4} $$

$$ f_{SRF} = \int_{t=0}^{t_f} \left(\frac{\|\mathbf{SRF}_R - \mathbf{SRF}_L\|}{\text{Body weight}} \right)^2 dt \tag{5} $$

where $\tau_i^{\lim}$ represents the torque range of the ith DOF. $\tau_i^{\lim} = |\tau_i^U - \tau_i^L|$ with τ_i^U and τ_i^U representing the ith joint's physiological lower and upper limits of the strength, respectively. $\mathbf{q}$, $\dot{\mathbf{q}}$, and $\ddot{\mathbf{q}}$ are joint angle, velocity, and acceleration vectors, respectively. The assisted STS motion starts at 0s and end at t_f seconds. With Obj_1, only dynamic effort is minimized, whereas with Obj_2 the objective is not only minimizing dynamic effort, but also minimizing the difference between right side and left side SRFs.

2.2.3 Constraints. Constraints include joint angle limits, joint torque limits, foot contact with the ground, chair height and contact, stability, initial and final postures, and initial and final joint velocity and acceleration [45], two additional groups of constraints are added. The first group is to ensure that each individual's middle of the right hand contacts the grab-rail bar placed on the right side during the entire motion. The information on the geometry of the bar and its location are provided by O'Meara and Smith [4]. The grab-rail bar is modeled as 0.50 m long with a minimum height of 0.80 m in the vertical orientation. The anterior position of the grab-rail bar is ranged from 0.40 m to 0.60 m, whereas the lateral position is kept in a range of 0.35 m to 0.55 m from the pelvis point. The second group of the additional constraints ensures that right hand SRF profiles have values equal to zero during the initial and the last instances of the motion in the A/P, M/L, and vertical directions [4,48]. The hand reaction force due to the contact is modeled with an unknown profile of an external load that has three components in A/P, M/L, and vertical axes. With this set of additional constraints, the virtual-individuals are limited to receive no assistance during the trunk flexion stage and at the final instance of the motion [48].

The constrained optimization problems with the given anthropometric information of the digital individuals are solved through the sequential quadratic programming in a commercial software-MATLAB® (The MathWorks Inc., Natick, MA) with parallel computing.

3 Results and Discussion

Assisted STS motions of healthy elderly virtual-individuals are predicted and two objective functions are tested for each case. After 20 simulations are completed, kinematic and kinetic results are compared with two different objective functions. The joint angle and right hand SRF profiles are shown only for one virtual-individual for the sake of simplicity. However, in the text and tables, results are shown for all the virtual-individuals.

Note that the virtual-group consists of healthy elderly virtual-individuals without any musculoskeletal abnormalities. As a result of the optimal location of the grab-rail bar, no significant difference is observed between two objective functions. With Obj_1, the optimal location of the grab-rail bar is predicted to be 0.41 (0.02) m to the right side of the sagittal plane, 0.51 (0.04) m anterior to the pelvis, and 0.98 (0.06) m above the ground. With Obj_2, the optimal location is predicted to be 0.40 (0.03) m to the right side of the sagittal plane, 0.52 (0.03) m anterior to the pelvis, and 0.99 (0.06) m above the ground.

In conjunction with the optimal location, the grab-rail reaction forces are predicted to be similar with Obj_1 and Obj_2. In Obj_1, rail-reaction forces are predicted to be 2.3 (0.7)% BW, 6.4 (1.2)% BW, and 3.8 (1.5)% BW in lateral, vertical, and anterior directions. With

Obj_2, these reaction forces are predicted to be 1.9 (1.3)% BW, 6.3 (1.2)% BW, and 3.2 (0.6)% BW. The average magnitude of reaction load from five different orientations and location combinations of a unilateral grab-rail bar was measured as ~4% BW in M/L, and ~6% BW in A/P and vertical directions in O'Meara and Smith [4]. An example of the rail reaction force profiles can be seen in Fig. 2. In this study, the M/L component of the rail-reaction force is the first component to reach a peak, followed by vertical and A/P components. The same trend was also observed in O'Meara and Smith [4] experimentally. Since the rail-reaction forces are predicted to be similar, rail-reaction force profiles are shown only from the predicted results with Obj_1.

Upper-body joint angle profiles of a healthy elderly virtual-individual in sagittal, frontal, and transverse planes can be seen in Fig. 3. Also, mean and standard deviation values of the upper-body peak joint angles can be seen in Table 1 with two different objective functions. As a result of the introduction of the grab-rail bar, no significant difference is observed in the upper-body peak joint angles between two objective functions in the sagittal plane. However, the required lateral trunk flexion angle to the right side and axial rotation in the transverse plane are significantly higher during assisted STS with both of the objective functions. With the introduction of the grab-rail bar, the healthy elderly virtual-individuals show no significant difference in the sagittal plane peak trunk joint angle, and yet, as measured experimentally by O'Meara and Smith [4], virtual-individuals flex their trunk laterally more. The axial rotation angle of the upper-body to the right side plays an important role with both Obj_1 and Obj_2 and has a significantly larger impact with the usage of a grab-rail bar. The only difference in the peak upper-body joint angles is observed in the lateral bending angle between the results of Obj_1 and Obj_2. Since the difference between the right side and the left side vertical SRFs is minimized with Obj_2, virtual-individuals tend to flex their trunk laterally less than that of with Obj1 to prevent excessive leaning laterally.

Lower-body joint angle profiles of a healthy elderly virtual-individual can be seen in Fig. 4. Mean and standard deviation values of the lower-body peak joint angles can also be seen in Table 2 with two different objective functions.

Similar to the upper-body joints, some differences are observed in the lower-body peak joint angles between Obj_1 and Obj_2. The differences observed in the sagittal plane peak joint angles of the lower limbs are not significant, however, it can be concluded that the joint coordination of both lower and upper extremities in the sagittal plane is not affected by the introduction of the grab-rail bar. Granted, peak joint angles of right hip adduction, left hip abduction, right hip internal rotation, and left hip external rotation are significantly higher during assisted STS maneuver that matches results from experimental study [4].

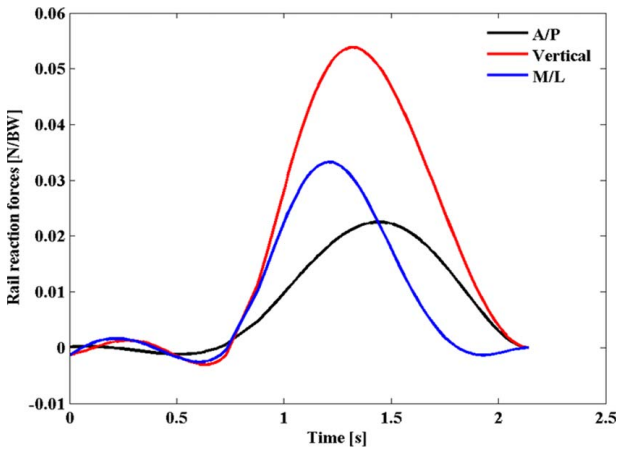

Fig. 2 Rail-reaction forces of a healthy elderly virtual-individual during an assisted STS task

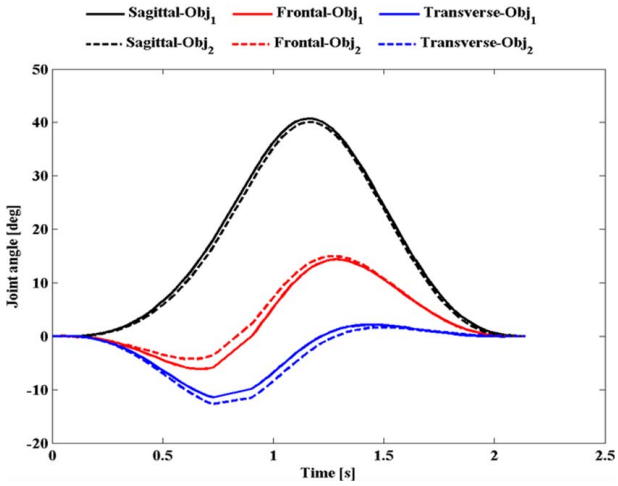

Fig. 3 Upper-body joint angle profiles of a healthy elderly virtual-individual during an assisted STS task

As noted earlier, initial foot locations play an important role in the overall performance. In Yang and Ozsoy [45], the prediction formulation resulted in both ankles dorsiflexed at the initial posture with angles of 23.22 (2.31) deg and 22.42 (3.11) deg for the right and left sides, respectively. The dorsiflexion of the ankle joints resulted in placing the right and left feet posterior to the knees, reducing the distance between the zero moment point (ZMP) and support region during an unassisted STS task. Since the initial ankle joint angles were predicted to be close to a human's physiological limit for a healthy elderly individual during an STS task without grab-rail support, ankle joint angles in the sagittal plane did not change until the seat-off instance and this result is consistent with experimental result in O'Meara and Smith [4]. With the introduction of the grab-rail bar, the prediction formulation results in initial joint angles that are less than the healthy elderly virtual-individuals' initial ankle joint angles during an STS task without the grab-rail support. Both ankle joints are dorsiflexed more during the trunk flexion stage of the motion and reach to peak at the seat-off instance as similar to those of the healthy elderly group without a unilateral grab-rail bar. It should also be noted that with the grab-rail bar, no significant differences are observed between the right and left side sagittal plane joint angles [4].

The upper-body and lower-body joint angular velocity profiles of a healthy elderly virtual-individual can be seen in Figs. 5 and 6. Mean and standard deviation values of the lower-body peak joint angles can be seen in Table 3 with two different objective functions. The same trend observed for joint angle profiles reoccurs in the joint angular velocity profiles.

With the introduction of the unilateral grab-rail bar, no significant differences are observed in the sagittal plane joint angle velocities in the lower and upper-body with both objective functions. Instead, the healthy elderly virtual-individuals tend to use the trunk on frontal

Table 1 Upper-body peak joint angles of healthy elderly individuals during an assisted STS task and comparison with unassisted case [45]

Joint angle (deg)		Obj_1	Obj_2
Trunk	Sagittal—flexion	44.87 (12.55)	44.50 (11.13)
	Frontal—left bend	5.20 (2.41)	**2.23 (0.97)**[b]
	Frontal—right bend	**9.46 (4.53)**[a]	**11.45 (3.90)**[a]
	Transverse—left rotate	2.55 (2.81)	1.88 (2.81)
	Transverse—right rotate	**7.73 (2.55)**[a]	**10.14 (7.54)**[a]

[a]Results are significantly different without assistance.
[b]Results are significantly different than those predicted with Obj_1.

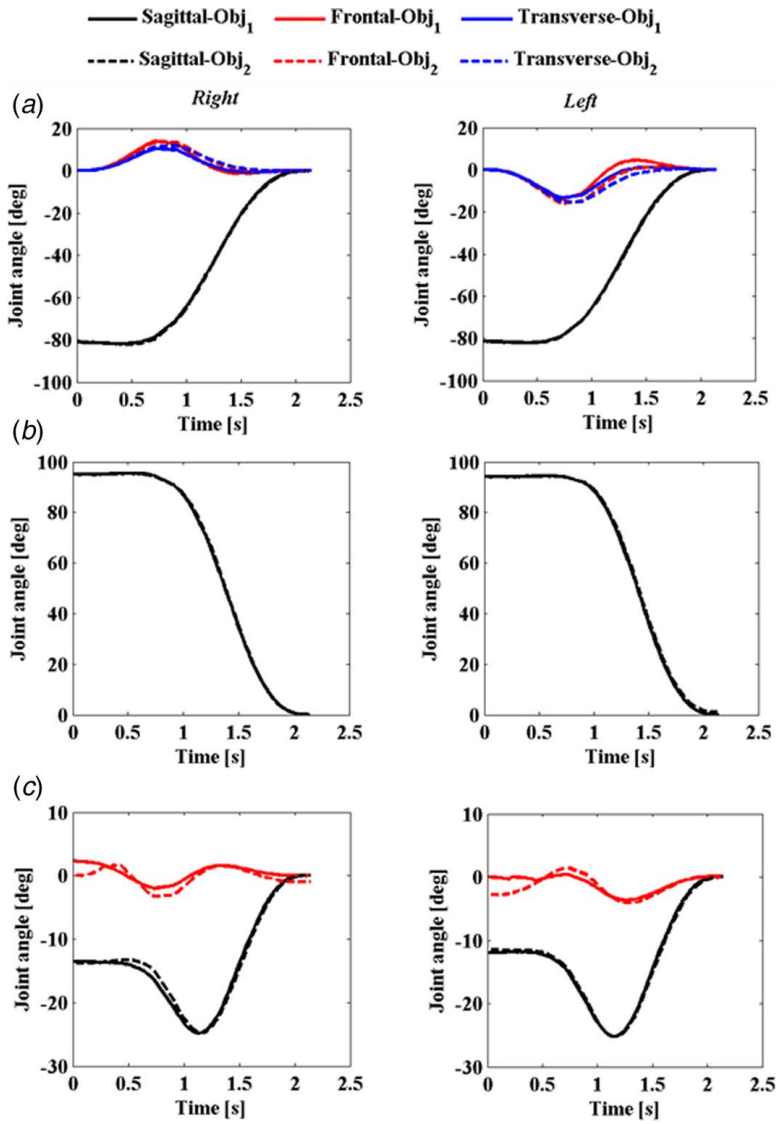

Fig. 4 Lower-body joint angle profiles of a healthy elderly virtual-individual during an assisted STS task: (*a*) hip, (*b*) knee, and (c) ankle

Table 2 Mean and standard deviation values of lower-body peak joint angles of healthy elderly virtual-individuals during an assisted STS task

Lower-body peak joint angles (deg)			Obj_1	Obj_2
Sagittal plane	Right	Hip flexion	84.35 (4.43)	83.82 (4.79)
		Knee flexion	98.61 (5.45)	99.76 (3.34)
		Ankle dorsiflexion	22.75 (2.56)	22.43 (2.45)
	Left	Hip flexion	84.65 (4.50)	83.73 (5.08)
		Knee flexion	97.57 (5.43)	98.63 (3.91)
		Ankle dorsiflexion	23.49 (2.35)	23.78 (1.95)
Frontal plane	Right	Hip adduction	**12.88 (2.51)**[a]	**14.77 (5.37)**[a]
		Hip abduction	2.52 (2.17)	0.68 (1.12)
		Ankle eversion	3.21 (1.17)	3.58 (1.74)
	Left	Hip adduction	3.66 (2.52)	**1.04 (1.02)**[b]
		Hip abduction	**14.10 (4.24)**[a]	**12.96 (5.64)**[a]
		Ankle inversion	**7.09 (1.64)**[a]	**5.08 (2.53)**[a,b]
Transverse plane	Right	Hip internal rotation	**11.52 (4.89)**[a]	**0.79 (0.80)**[a]
		Hip external rotation	1.33 (1.26)	0.79 (0.80)
	Left	Hip internal rotation	0.17 (0.18)	0.07 (0.14)
		Hip external rotation	**13.77 (4.04)**[a]	**15.72 (7.47)**[a]

[a]Results are significantly different without assistance.
[b]Results are significantly different than those predicted with Obj_1.

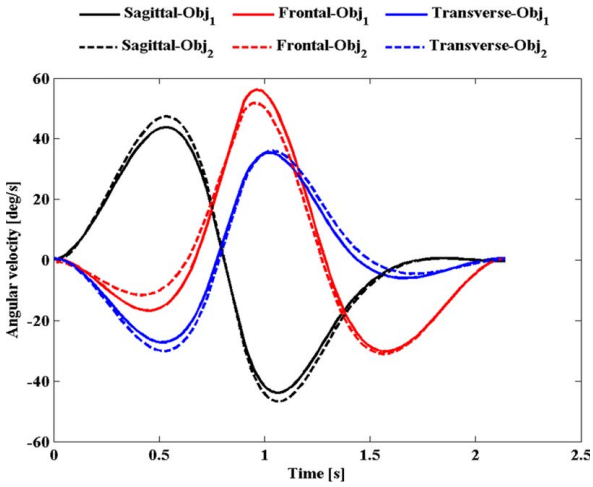

Fig. 5 Upper-body joint velocity profiles of a healthy elderly individual during an assisted STS task

and transverse planes significantly more with the introduction of a grab-rail. It suggests that the unilateral grab-rail enhances the lateral and anterior propulsion during the assisted STS maneuver, which is consistent with the findings of O'Meara and Smith [4]. The only difference between the peak upper-body joint velocity results of Obj_1 and Obj_2 is seen in the lateral flexion of the trunk. With Obj_2, the required trunk lateral flexion velocity decreases from 47.46 (9.92) deg/s to 36.54 (8.93) as compared with Obj_1. It should be noted that no significant differences are observed in the peak shoulder angles and angular velocities (abduction–adduction, internal–external rotation, and flexion–extension) between Obj_1 and Obj_2.

Although peak lower and upper-body joint angles in the sagittal plane are not affected by the introduction of the grab-rail bar, peak joint angular velocities are significantly different. For instance, with the unilateral grab-rail bar, the right knee extension peak angular velocity is significantly less, whereas right and left ankle plantar-flexion and dorsiflexion velocities are significantly higher. No significant differences are observed in right and left hip extensor velocities and left knee extensor velocity. Likewise, the healthy elderly virtual-individuals have higher velocities in the right and

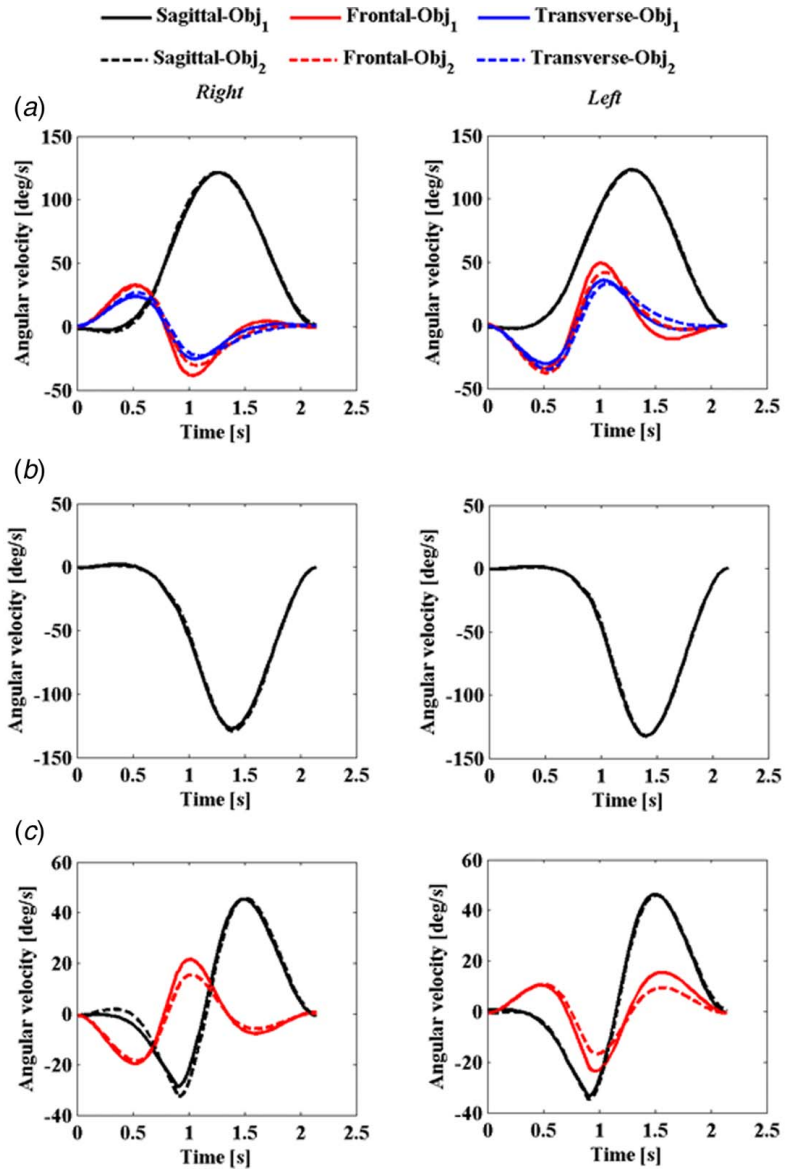

Fig. 6 Lower-body joint velocity profiles of a healthy elderly virtual-individual during an assisted STS task: (*a*) hip, (*b*) knee, and (*c*) ankle

Table 3 Mean and standard deviation values of lower-body peak joint velocities of elderly virtual-individuals during an assisted STS task [45]

Peak joint angular velocities (deg/s)			Obj_1	Obj_2
Sagittal plane	Right	Hip extension	130.07 (14.59)	122.41 (11.86)[a]
		Knee extension	**127.36 (4.73)**[a]	**125.44 (6.54)**[a]
		Ankle plantarflexion	**37.36 (4.86)**[a]	**36.80 (3.60)**[a]
	Left	Hip extension	132.30 (14.26)	**123.50 (10.86)**[a]
		Knee extension	129.44 (6.91)	129.10 (5.13)
		Ankle plantarflexion	**39.31 (5.55)**[a]	**39.28 (3.83)**[a]
Frontal plane	Right	Hip adduction	**32.08 (11.52)**[a]	**29.91 (11.10)**[a]
		Hip abduction	**38.37 (10.40)**[a]	**32.70 (11.43)**[a]
		Ankle inversion	**21.85 (4.02)**[a]	**17.44 (4.75)**[a,b]
		Ankle eversion	**17.49 (4.21)**[a]	**15.49 (2.83)**[a]
	Left	Hip adduction	**43.70 (12.62)**[a]	**31.38 (13.32)**[a,b]
		Hip abduction	**32.41 (9.23)**[a]	**31.87 (10.92)**[a]
		Ankle inversion	**29.91 (8.60)**[a]	**28.11 (11.15)**[a]
		Ankle eversion	**28.30 (8.83)**[a]	**29.61 (12.66)**[a]
Transverse plane	Right	Hip internal rotation	**25.36 (12.31)**[a]	**29.96 (13.82)**[a]
		Hip external rotation	**23.62 (8.11)**[a]	**26.25 (11.61)**[a]
	Left	Hip internal rotation	**29.91 (8.60)**[a]	**28.11 (11.15)**[a]
		Hip external rotation	**28.30 (8.83)**[a]	**29.61 (12.66)**[a]

[a]Results are significantly different without assistance.
[b]Results are significantly different than those predicted with Obj_1.

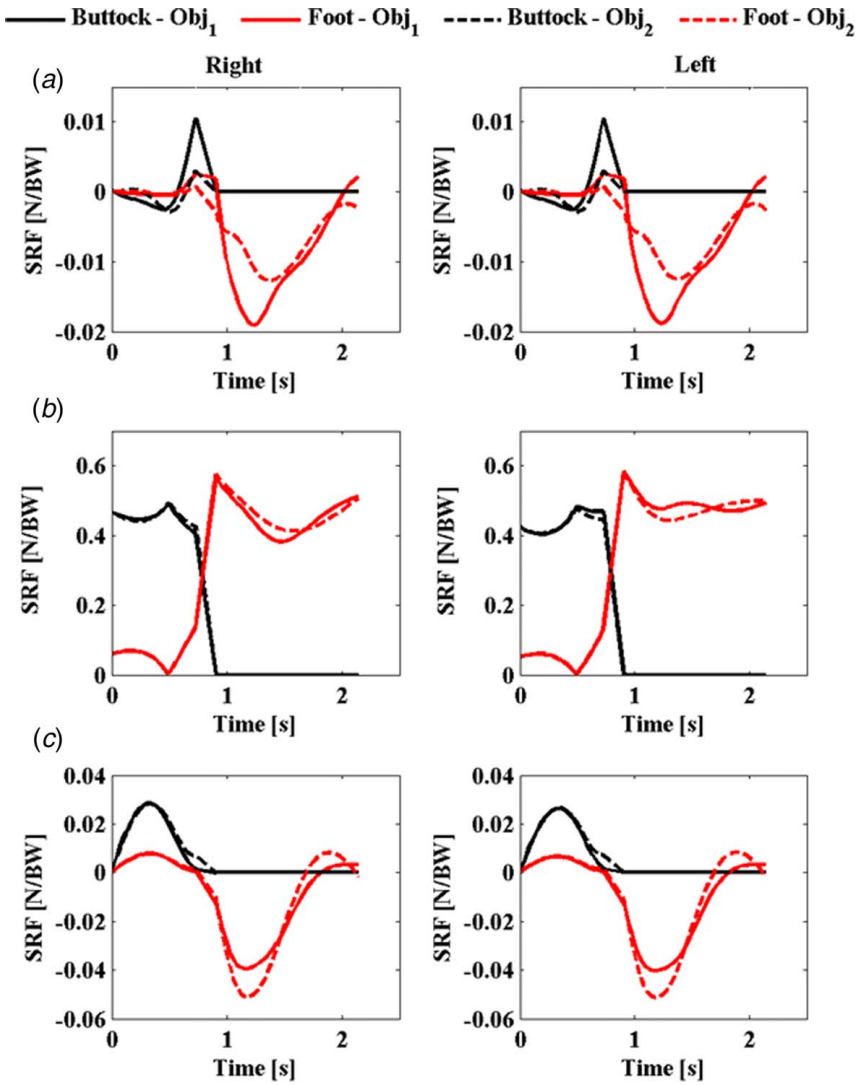

Fig. 7 SRF profiles of a healthy elderly virtual-individual during an assisted STS maneuver: (*a*) M/L, (*b*) vertical, and (*c*) A/P

Table 4 Normalized mean and standard deviation values of peak SRFs of healthy elderly virtual-individuals (% N/BW) at the feet during an assisted STS task

Side	Component	Unassisted STS [45]	Assisted STS Obj_1	Assisted STS Obj_2
Right	Vertical	55.1 (2.1)	58.7 (2.9)[a]	57.0 (2.2)
	Posterior	3.9 (0.8)	4.7 (2.0)	4.2 (1.1)
	Anterior	1.2 (0.9)	1.0 (0.7)	0.7 (0.2)
	Lateral	0.6 (0.2)	0.5 (0.4)	**0.1 (0.2)**[a,b]
	Medial	0.8 (0.4)	**2.8 (1.4)**[a]	**1.5 (0.4)**[a,b]
Left	Vertical	58.1 (4.4)	56.4 (4.0)	57.6 (2.1)
	Posterior	3.7 (0.6)	5.2 (2.7)	4.3 (1.1)
	Anterior	1.2 (0.8)	0.9 (0.7)	0.7 (0.2)
	Lateral	0.6 (0.3)	0.5 (0.4)	**0.1 (0.2)**[a,b]
	Medial	0.4 (0.3)	**2.7 (1.3)**[a]	**1.5 (0.4)**[a,b]

[a]Results are significantly different without assistance.
[b]Results are significantly different than those predicted with Obj_1.

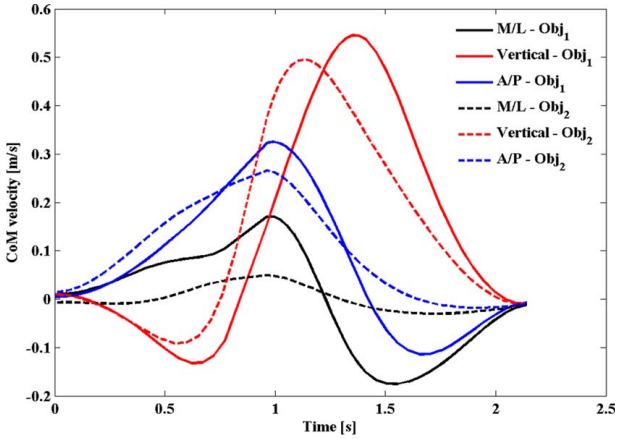

Fig. 8 CoM velocity profiles of a healthy elderly virtual-individual during an assisted STS task

left hip adduction, adduction, internal and external rotations, and ankle inversion and eversion. The only significant differences between the peak lower-body joint velocities are seen in right ankle inversion and left hip abduction with Obj_1 and Obj_2.

SRF profiles can be seen in Fig. 7 in A/P, vertical, and M/L directions. The healthy elderly virtual-individuals' normalized mean and standard deviation values of the SRFs at the feet can be seen in Table 4 for both objective functions. As compared with an unassisted STS, the right foot vertical SRF experienced an increase whereas the magnitude of the left foot vertical SRF remains almost the same with Obj_1. Unlike the experimental measurements of peak SRFs at the feet [4], where an increase in the right foot peak posterior SRF and a decrease in the left side were measured, no significant differences are observed in the peak posterior SRFs in this study. Granted, trends observed in vertical SRFs are consistent with O'Meara and Smith [4]. The only difference between the two objective functions is seen in the peak SRFs in the M/L direction. This highlights that peak right and left side SRFs in the lateral and medial directions are experienced reductions with Obj_2.

Sagittal plane joint torques are shown in Table 5 with normalized means and standard deviation values. Also in the same table, a comparison between assisted and unassisted STS maneuver joint torques of the healthy elderly virtual-individuals is provided. The effect of the unilateral grab-rail on the joint torques was observed as reductions in right ankle dorsiflexion and left knee extension and an increase in the right knee extension [4]. In this study, as a result of the comparison between assisted and unassisted STS maneuvers, the only significant difference observed is in the left knee extension peak torque. The left knee experiences a reduction with the unilateral grab-rail. No significant differences are observed in sagittal plane joint torques between Obj_1 and Obj_2.

In terms of the upper-body joint torques, no difference is recorded in the peak trunk flexion torque in the sagittal plane between Obj_1 and Obj_2. The peak of the upper-body joint torques in the transverse and frontal planes experiences significant increases with the introduction of the grab-rail bar.

A healthy elderly individual's center of mass (CoM) velocity profiles with two different objective functions can be seen in Fig. 8. Mean and standard deviation values of peak CoM velocity, CoM displacement, and CoM-ZMP excursion during unassisted and assisted STS tasks can also be seen in Table 6. In terms of the peak CoM velocity, a significant difference is noted in the M/L component only with Obj_1. With Obj_2, the peak M/L component of CoM velocity is predicted to be similar with an unassisted STS case. The healthy elderly virtual-individuals are predicted to lean their upper-body to the right side during an assisted STS task with both Obj_1 and Obj_2. It is crucial to mention that no significant differences are observed in A/P and vertical components of CoM velocity between two objective functions. In terms of the peak CoM displacement, it is predicted that the A/P component experiences an increase with both objective functions, which is consistent with O'Meara and Smith [4] and Schultz et al. [2]. No significant difference is seen in the M/L component of peak CoM displacement. The M/L component of the CoM-ZMP excursion experiences an increase with the introduction of the unilateral grab-rail bar, while A/P is not affected.

In conclusion, it can be said that the trends observed in predicted kinematics and kinetics between unassisted and assisted STS tasks are similar to the experimental results of O'Meara and Smith [4] with both of the objective functions. Sagittal plane kinematics and kinetics are not affected by the introduction of the grab-rail bar, whereas some significant differences are seen in the M/L and A/P components of kinematics and kinetics. It is important to note that it would be impossible to assume that all human beings prefer to stand up from a chair by using either one of the performance criterion (objective functions). But it seems like the formulation with Obj_1 can reflect the systematic asymmetry in kinematics and kinetics better than Obj_2. The increase in the peak CoM displacement shows that the healthy elderly group places a priority to the stability during an assisted STS task. Finally, the proposed formulation shows that the

Table 5 Mean and standard deviation of sagittal plane torques of healthy elderly virtual-individuals during unassisted and assisted STS maneuvers (N m/kg m)

	Unassisted STS [45]		Assisted STS Obj_1		Assisted STS Obj_2	
	Right	Left	Right	Left	Right	Left
Hip extension	0.49 (0.11)	0.45 (0.07)	0.45 (0.10)	0.53 (0.10)	0.49 (0.11)	0.51 (0.11)
Knee extension	0.58 (0.05)	0.59 (0.04)	0.55 (0.08)	**0.51 (0.06)**[a]	**0.51 (0.07)**[a]	**0.55 (0.07)**[a]
Ankle plantarflexion	0.27 (0.12)	0.25 (0.10)	0.21 (0.12)	0.18 (0.08)	0.20 (0.07)	0.18 (0.07)
Ankle dorsiflexion	0.14 (0.05)	0.13 (0.05)	0.14 (0.03)	0.13 (0.03)	0.13 (0.03)	0.13 (0.03)

[a]Results are significantly different without arm support.

Table 6 Mean and standard deviation of peak CoM velocity, CoM displacement, and CoM-ZMP excursion of healthy elderly virtual-individuals during unassisted and assisted STS tasks

	Component	Unassisted STS [45]	Assisted STS Obj_1	Assisted STS Obj_2
Peak CoM velocity (m/s)	M/L	0.024 (0.009)	**0.071 (0.043)**[a]	**0.033 (0.020)**[b]
	Vertical	0.460 (0.051)	0.473 (0.049)	0.468 (0.051)
	A/P	0.253 (0.047)	0.300 (0.070)	0.276 (0.065)
Peak CoM displacement (m)	M/L	0.019 (0.015)	0.034 (0.025)	0.028 (0.019)
	A/P	0.189 (0.028)	**0.255 (0.064)**[a]	**0.229 (0.050)**[a]
CoM-ZMP excursion (m)	M/L	0.007 (0.003)	**0.029 (0.007)**[a]	**0.026 (0.005)**[a]
	A/P	0.045 (0.014)	0.041 (0.012)	0.040 (0.010)

[a]Results are significantly different without assistance.
[b]Results are significantly different than those predicted with Obj_1.

placement of the grab-rail bar on the right side results in a significant decrease in the left knee joint torque. Therefore, it may suggest that the vertical unilateral grab-rail bar should be installed on the opposite side of the weak knee for the elderly to reduce potential injury risk for STS task.

Assisted STS motion prediction formulation developed in this paper provides a tool to easily check cause and effect in biomechanics field. Therefore, this formulation could be used in many applications: development of subject-specific exoskeletons for elderly individuals who suffer difficulties during STS tasks to provide extra strength in the weak side of the body, the development of a microelectromechanical system for fall detection during STS tasks whenever the predicted kinematics and kinetics are abnormal, and the design of assistive devices in the burgeoning rehabilitation in the field of robotics to understand the human and robot interaction.

Limitations of the developed prediction formulation include the following: (1) the duration of the assisted STS motion is considered to be 2.14 s for healthy elderly individuals. Although it is known that the introduction of the grab-rail bar has no effect on the total duration of the motion for the healthy elderly group. As one knows that the developed formulation is capable of time optimization, it can only optimize intermediate knots for the optimal stage durations within a predefined total duration of the motion. However, the final knot cannot be treated as a design variable due to the following reason: the peak sagittal plane joint torques are mostly contributed by gravitational components and torque due to inertia components having significantly smaller values during normal speed STS tasks. As a result of the time optimization, including the optimization of the final knot, the optimization procedure tries to minimize inertial component as well. Thus, it yields an optimal value of the final knot that converges to the upper limit. (2) Joint angle limits for each subject is given to the optimization problem with identical values. Although the values of the angle limits are taken from the literature, they represent an average range. However, in reality each individual has different range of motions at each joint. (3) Inertial parameters, center of mass locations, and segmental masses of each link are predicted through regression equations found in literature which are derived from the elderly subjects. (4) Although torque limit values are subject-specific in this study, they are either taken from the literature with normalized values with respect to the subject's height and weight or predicted through regression equations as a function of age, gender, height, and weight. However, in reality, no one can neither guarantee nor prove that two subjects with identical anthropometric measurements would have the same joint strengths. (5) The motion is modeled in the joint space due to the advantages of computational efficiency, robustness, and stability. However, the skeletal model is missing muscle activation information in the literature. (6) The proposed simulation results are compared with only one available published paper and no experiments have been conducted in this study. (7) Only two objective functions have been investigated. In future studies, the effect of the introduction of the grab-rail bar on the muscle activities can and should be studied and experiments will be carried out to validate the model.

4 Conclusion

This study extended our previous formulation for unassisted STS motion prediction to predict spatial assisted STS motion while the grab-rail bar was considered to be installed on the right side of the virtual-individuals with a vertical orientation for healthy elderly virtual-individuals. Since the unilateral grab-rail bar brings in systematic asymmetry to kinematics and kinetics results, two different objective functions were tested. As a result, the significant changes observed in the kinematics and kinetics especially in the frontal and transverse planes between assisted and unassisted STS tasks of the healthy elderly virtual-individuals matched well with those observed in an experimental study found in the literature. It concluded, as well, that the first objective function could reflect the systematic asymmetry brought by the unilateral grab-rail bar better than the second objective function because the second objective function minimizes the difference between left and right feet support forces. Furthermore, it is shown that the healthy elderly virtual-individuals place a priority to stability during assisted STS tasks by increasing the peak CoM displacement in the anterior direction.

Acknowledgment

This work was partially supported by National Science Foundation (CBET 0926549).

Conflict of Interest

There are no conflicts of interest.

Data Availability Statement

The datasets generated and supporting the findings of this paper are obtainable from the corresponding author upon reasonable request.

References

[1] Dawson, D. A., Hendershot, G. E., and Fulton, J. P., 1987, *Aging in the Eighties: Functional Limitations of Individuals age 65 Years and Over*, Advance Data From Vital and Health Statistics, No. 133, DHHS Pub. No. (PHS) 87–1 250, National Center for Health Statistics, Public Health Service, Hyattaville, MD.
[2] Schultz, A. B., Alexander, N. B., and Ashton-Miller, J. A., 1992, "Biomechanical Analyses of Rising From a Chair," J. Biomech., **25**(12), pp. 1383–1391.
[3] Census Bureau, U. S., 2017, Population Division, Annual Estimates of the Resident Population for Selected Age Groups by Sex for the United States,

States, Counties, and Puerto Rico Commonwealth and Municipios: April 1, 2010 to July 1, 2016. Release Date: June 2017.
[4] O'Meara, D. M., and Smith, R. M., 2006, "The Effects of Unilateral Grab Rail Assistance on the Sit-to-Stand Performance of Older Aged Adults," Hum. Mov. Sci., **25**(2), pp. 257–274.
[5] Riley, P. O., Schenkman, M. L., Mann, R. W., and Hodge, W. A., 1991, "Mechanics of a Constrained Chair-Rise," J. Biomech., **24**(1), pp. 77–85.
[6] Gross, M. M., Stevenson, P. J., Charette, S. L., Pyka, G., and Marcus, R., 1998, "Effect of Muscle Strength and Movement Speed on the Biomechanics of Rising From a Chair in Healthy Elderly and Young Women," Gait Posture, **8**(3), pp. 175–185.
[7] Kralj, A., Jaeger, R. J., and Munih, M., 1990, "Analysis of Standing Up and Sitting Down in Humans: Definitions and Normative Data Presentation," J. Biomech., **23**(11), pp. 1123–1138.
[8] Pai, Y.-C., and Rogers, M. W., 1991, "Speed Variation and Resultant Joint Torques During Sit-to-Stand," Arch. Phys. Med. Rehabil., **72**(11), pp. 881–885.
[9] Pai, Y.-C., Naughton, B. J., Chang, R. W., and Rogers, M. W., 1994, "Control of Body Centre of Mass Momentum During Sit-to-Stand Among Young and Elderly Adults," Gait Posture, **2**(2), pp. 109–116.
[10] Lord, S. R., Murray, S. M., Chapman, K., Munro, B., and Tiedemann, A., 2002, "Sit-to-Stand Performance Depends on Sensation, Speed, Balance, and Psychological Status in Addition to Strength in Older People," J. Gerontol. A Biol. Sci. Med. Sci., **57**(8), pp. M539–43.
[11] Dehail, P., Bestaven, E., Muller, F., Mallet, A., Robert, B., Bourdel-Marchasson, I., and Petit, J., 2007, "Kinematic and Electromyographic Analysis of Rising From a Chair During a 'Sit-to-Walk' Task in Elderly Subjects: Role of Strength," Clin. Biomech., **22**(10), pp. 1096–1103.
[12] Yoshioka, S., Nagano, A., Hay, D. C., and Fukashiro, S., 2009, "Biomechanical Analysis of the Relation Between Movement Time and Joint Moment Development During a Sit-to-Stand Task," Biomed. Eng. Online, **8**(2), p. 27.
[13] Fujimoto, M., and Chou, L.-S., 2012, "Dynamic Balance Control During Sit-to-Stand Movement: An Examination With the Center of Mass Acceleration," J. Biomech., **45**(3), pp. 543–548.
[14] Mourey, F., Grishin, A., D'Athis, P., Pozzo, T., and Stapley, P., 2000, "Standing Up From a Chair as a Dynamic Equilibrium Task: A Comparison Between Young and Elderly Subjects," J. Gerontol. A Biol. Sci. Med. Sci., **55**(9), pp. B425–B431.
[15] Lundin, T. M., Grabiner, M. D., and Jahnigen, D. W., 1995, "On the Assumption of Bilateral Lower Extremity Joint Moment Symmetry During the Sit-to-Stand Task," J. Biomech., **28**(1), pp. 109–112.
[16] Gillette, J. C., and Stevermer, C. A., 2012, "The Effects of Symmetric and Asymmetric Foot Placements on Sit-to-Stand Joint Moments," Gait Posture, **35**(1), pp. 78–82.
[17] Gilleard, W., Crosbie, J., and Smith, R., 2008, "Rising to Stand From a Chair: Symmetry, and Frontal and Transverse Plane Kinematics and Kinetics," Gait Posture, **27**(1), pp. 8–15.
[18] Gilleard, W., Crosbie, J., and Smith, R., 2008, "A Longitudinal Study of the Effect of Pregnancy on Rising to Stand From a Chair," J. Biomech., **41**(4), pp. 779–787.
[19] Hughes, M. A., Weiner, D. K., Schenkman, M. L., Long, R. M., and Studenski, S. A., 1994, "Chair Rise Strategies in the Elderly," Clin. Biomech., **9**(3), pp. 187–192.
[20] Roy, G., Nadeau, S., Gravel, D., Malouin, F., McFadyen, B. J., and Piotte, F., 2006, "The Effect of Foot Position and Chair Height on the Asymmetry of Vertical Forces During Sit-to-Stand and Stand-to-sit Tasks in Individuals With Hemiparesis," Clin. Biomech., **21**(6), pp. 585–593.
[21] Kawagoe, S., Tajima, N., and Chosa, E., 2000, "Biomechanical Analysis of Effects of Foot Placement With Varying Chair," J. Orthop. Sci., **5**(2), pp. 124–133.
[22] Rodosky, M. W., Andriacchi, T. P., and Andersson, G. B., 1989, "The Influence of Chair Height on Lower Limb Mechanics During Rising," J. Orthop. Res., **7**(2), pp. 266–271.
[23] Burdett, R. G., Habasevich, R., Pisciotta, J., and Simon, S. R., 1985, "Biomechanical Comparison of Rising From Two Types of Chairs," Phys. Ther., **65**(8), pp. 1177–1183.
[24] Arborelius, U. P., Wretenberg, P., and Lindbikikerg, F., 1992, "The Effects of Armrests and High Seat Heights on Lower-Limb Joint Load and Muscular Activity During Sitting and Rising," Ergonomics, **35**(11), pp. 1377–1391.
[25] Anglin, C., and Wyss, U. P., 2000, "Arm Motion and Load Analysis of Sit-to-Stand, Stand-to-Sit, Cane Walking and Lifting," Clin. Biomech., **15**(6), pp. 441–448.
[26] Kamnik, R., Bajd, T., and Kralj, A., 1999, "Functional Electrical Stimulation and Arm Supported Sit-to-Stand Transfer After Paraplegia: A Study of Kinetic Parameters," Artif. Organs, **23**(5), pp. 413–417.
[27] Papa, E., and Cappozzo, A., 2000, "Sit-to-Stand Motor Strategies Investigated in Able-Bodied Young and Elderly Subjects," J. Biomech., **33**(9), pp. 1113–1122.
[28] Najafi, B., Aminian, K., Loew, F., Blanc, Y., and Robert, P. A., 2002, "Measurement of Stand-Sit and Sit-Stand Transitions Using a Miniature Gyroscope and Its Application in Fall Risk Evaluation in the Elderly," IEEE Trans. Biomed. Eng., **49**(8), pp. 843–851.
[29] Ikeda, E. R., Schenkman, M. L., Riley, P. O., and Hodge, W. A., 1991, "Influence of Age on Dynamics of Rising From a Chair," Phys. Ther., **71**(6), pp. 473–481.
[30] Shepherd, R. B., and Koh, H. P., 1996, "Some Biomechanical Consequences of Varying Foot Placement in Sit-to-Stand in Young Women," Scand. J. Rehabil. Med., **28**(2), pp. 79–88.
[31] Su, F. C., Lai, K. A., and Hong, W. H., 1998, "Rising From Chair After Total Knee Arthroplasty," Clin. Biomech., **13**(3), pp. 176–181.
[32] Talis, V. L., Grishin, A. A., Solopova, I. A., Oskanyan, T. L., Belenky, V. E., and Ivanenko, Y. P., 2008, "Asymmetric Leg Loading During Sit-to-Stand, Walking and Quiet Standing in Patients After Unilateral Total Hip Replacement Surgery," Clin. Biomech., **23**(4), pp. 424–433.
[33] Coghlin, S. S., and McFadyen, B. J., 1994, "Transfer Strategies Used to Rise From a Chair in Normal and Low Back Pain Subjects," Clin. Biomech., **9**(2), pp. 85–92.
[34] Mizner, R. L., and Snyder-Mackler, L., 2005, "Altered Loading During Walking and Sit-to-Stand is Affected by Quadriceps Weakness After Total Knee Arthroplasty," J. Orthop. Res., **23**(5), pp. 1083–1090.
[35] Mak, M. K. Y., Levin, O., Mizrahi, J., and Hui-Chan, C. W. Y., 2003, "Joint Torques During Sit-to-Stand in Healthy Subjects and People With Parkinson's Disease," Clin. Biomech., **18**(3), pp. 197–206.
[36] Bahrami, F., Riener, R., Jabedar-Maralani, P., and Schmidt, G., 2000, "Biomechanical Analysis of Sit-to-Stand Transfer in Healthy and Paraplegic Subjects," Clin. Biomech., **15**(2), pp. 123–133.
[37] Sibella, F., Galli, M., Romei, M., Montesano, A., and Crivellini, M., 2003, "Biomechanical Analysis of Sit-to-Stand Movement in Normal and Obese Subjects," Clin. Biomech., **18**(8), pp. 745–750.
[38] Lou, S.-Z., Chou, Y.-L., Chou, P.-H., Lin, C.-J., Chen, U.-C., and Su, F.-C., 2001, "Sit-to-Stand at Different Periods of Pregnancy," Clin. Biomech., **16**(3), pp. 194–198.
[39] Pandy, M. G., Garner, B. A., and Anderson, F. C., 1995, "Optimal Control of Non-Ballistic Muscular Movements: A Constraint-Based Performance Criterion for Rising From a Chair," ASME J. Biomech. Eng., **117**(1), pp. 15–26.
[40] Domire, Z. J., 2004, "A Biomechanical Analysis of Maximum Vertical Jumps and Sit-to-Stand," Ph.D. dissertation, Pennsylvania State University.
[41] Norman-Gerum, V., and McPhee, J., 2018, "Constrained Dynamic Optimization of Sit-to-Stand Motion Driven by Bezier Curves," ASME J. Biomech. Eng., **140**(12), p. 121011.
[42] Kuželički, J., Žefran, M., Burger, H., and Bajd, T., 2005, "Synthesis of Standing-Up Trajectories Using Dynamic Optimization," Gait Posture, **21**(1), pp. 1–11.
[43] Mughal, A., and Iqbal, K., 2010, "3D Bipedal Model With Holonomic Constraints for the Decoupled Optimal Controller Design of the Biomechanical Sit-to-Stand Maneuver," ASME J. Biomech. Eng., **132**(4), p. 041010.
[44] Robert, T., Causse, J., and Monnier, G., 2013, "Estimation of External Contact Loads Using an Inverse Dynamics and Optimization Approach: General Method and Application to Sit-to-Stand Maneuvers," J. Biomech., **46**(13), pp. 2220–2227.
[45] Yang, J., and Ozsoy, B., 2020, "Three Dimensional Unassisted Sit-to-Stand Prediction for Virtual Healthy Young and Elderly Individuals," Multibody Syst. Dyn., **49**(1), pp. 33–52.
[46] Gordon, C. C., Churchill, T., Clauser, C. E., Bradtmiller, B., McConville, J. T., Tebbetts, I., and Walker, R. A., 1989, 1988 Anthropometric Survey of U.S. Army Personnel: Methods and Summary Statistics, Final Report (NATICK/TR-89/027), U.S. Army Natick Research, Development and Engineering Center, Natick, MA.
[47] McConville, J., Clauser, C., and Churchill, T., 1980, *Anthropometric Relationships of Body and Body Segment Moments of Inertia*, Anthropology Research Project INC, Yellow Springs, OH.
[48] O'Meara, D. M., and Smith, R. M., 2005, "Differences Between Grab Rail Position and Orientation During the Assisted Sit-to-Stand for Able-Bodied Older Adults," J. Appl. Biomech., **21**(1), pp. 57–71.